 doi:10.20944/preprints202104.0464.v1

Type of the Paper (Article)

Macrophage-Derived Small Exosomes: Efficient Transmission and Cytotoxicity to Cancer Cells

Yanyin Lu [1,2], Takanori Eguchi [1,3,*], Chiharu Sogawa [1,4], Eman A. Taha [1,5,6], Toshiki Nara [7], Manh Tien Tran[1], Peng-gong Wei [1,8], Shiro Fukuoka [1,9], Takuya Miyawaki [2], Kuniaki Okamoto [1]

1 Department of Dental Pharmacology, Okayama University Graduate School of Medicine, Dentistry and Pharmaceutical Sciences, Okayama 700-8525, Japan; riku21@s.okayama-u.ac.jp, trantienmanh1508@gmail.com, k-oka@okayama-u.ac.jp
2 Department of Dental Anesthesiology, Okayama University Graduate School of Medicine, Dentistry and Pharmaceutical Sciences, Okayama 700-8525, Japan; miyawaki@md.okayama-u.ac.jp
3 Advanced Research Center for Oral and Craniofacial Sciences, Okayama University Graduate School of Medicine, Dentistry and Pharmaceutical Sciences, Okayama, Japan
4 Current affiliation: Department of Clinical Engineering, Faculty of Life Sciences, Hiroshima Institute of Technology, Hiroshima 731-5193, Japan; c.sogawa.3b@cc.it-hiroshima.ac.jp
5 Department of Biochemistry, Ain Shams University Faculty of Science, Cairo 11566, Egypt.
6 Current affiliation: Center for iPS Cell Research and Application (CiRA), Kyoto University, Kyoto, Japan; eman.taha@cira.kyoto-u.ac.jp
7 Research Program for Undergraduate Students, Okayama University Dental School, Okayama 700-8525, Japan; pps64qnw@s.okayama-u.ac.jp
8 O-NECUS program, Okayama University Dental School. Department of Endodontics, School of Stomatology, China Medical University, Shenyang 110002, China; 1123044239@qq.com
9 Department of Orthopaedic Surgery, Okayama University Graduate School of Medicine, Dentistry and Pharmaceutical Sciences, Okayama 700-8558, Japan; pkbs3srr@okayama-u.ac.jp
* Correspondence: eguchi@okayama-u.ac.jp; Tel.: +81-86-235-6661

Abstract: Tumor-associated macrophages are a key component in the tumor microenvironment, secreting extracellular vesicles (EVs) such as exosomes and other various factors for intercellular communication. However, macrophage-derived EVs heterogeneity and their cytotoxicity to cancer cells has not been well understood. Here, we aimed to separately isolate various types of macrophage-EVs by size exclusion chromatography (SEC) method and investigate EV transmission and cytotoxicity to oral cancer cells. For fluorescence-labeling of cellular and EV membranes, palmitoylation signal-fused GFP and tdTomato were expressed in THP-1 monocytic cells and HSC-3 oral cancer cells, respectively. We found that fluorescence-labeled EVs secreted by macrophages were highly transmissive to oral cancer cells than those from parental monocytic cells. In a co-culture system and conditioned medium (CM), a macrophage-secreted unidentified factor was cytotoxic to oral cancer cells. We fractionated macrophage-derived EVs by the SEC method and performed western blotting to characterize various EV types. Three fractions were characterized: small exosomes (EXO-S: < 50 nm) fraction containing HSP90α, HSP90β, CD63 (EV marker) and β-actin; large exosomes (EXO-L: 50-200 nm) fraction containing CD9 (EV marker) and HSP90β; large EVs (100-500 nm) fraction. Notably, the macrophage-derived small exosomes fraction was cytotoxic to oral cancer cells, while large exosomes and large EVs were not. Therefore, it was implicated that macrophage-derived small exosomes are cytotoxic with high transmission potential to cancer cells.

Keywords: tumor-associated macrophage; exosomes; extracellular vesicles; heat shock proteins; oral cancer; fluorescent labeling of exosomes

1. Introduction

Extracellular vesicles (EVs) are small particles surrounded by lipid membrane, released by cells of diverse organisms, including eukaryotes and prokaryotic cells. In pluricellular organisms, EVs exist in different body fluids such as blood, urine, saliva, bile, ascites, amniotic fluid, breast milk, pleural ascites, synovial fluid, and cerebral spinal

fluid.[1] EVs contain various molecular cargo types, including proteins, nucleic acids, lipids, minerals, and metabolites[1–3]. Earlier studies classified EVs into three types: (1) exosomes (50 to 200 nm) originated from the endosome, (2) ectosomes, also called microvesicles or microparticles (200 nm to 1,000 nm) generated by budding and shedding of the plasma membrane of cells, (3) apoptotic bodies (1–5 μm), also known as apoptosome, originated via blebbing of the plasma membrane[4–6]. Additionally, non-membranous nanoparticles termed exomeres (~35 nm) involve metabolic enzymes and microtubule, hypoxia, coagulation proteins, glycosylation, and mTOR signaling[7]. Other types of vesicles have been reported, such as oncosomes (100 to 400 nm), large oncosomes (1–10 μm)[8,9], matrix vesicles[10,11], migrasomes[12] (50 nm to 3 μm), exopheres (~4 μm), and bacterial outer membrane vesicles (OMV)[13–15].

EVs are also classified by their size, for example, large EVs (L-EVs; e.g., 200-2000 nm) and small EVs (S-EVs; e.g., 50–200 nm) depending on the context of the works[3,16] S-EVs often contain exosomes, while L-EVs contain apoptotic bodies. Moreover, a previous study classified exosomes into larger exosomes (Exo-L, 90-120nm) and smaller exosomes (Exo-S 60-80 nm)[7]. Exosomes usually contain tetraspanins such as CD9 and CD63, used as protein biomarkers to demonstrate the exosomes' existence. Heat shock proteins (HSPs) are the regular components of EVs, while vesicle-free, extracellular HSPs have also been found[17–20].

Many methods have been developed for EV preparation, including ultracentrifugation (UC) method[21], filter centrifugation (FC), size exclusion chromatography (SEC)[22,23], affinity purification (AP), immunoprecipitation (IP), sucrose cushion ultracentrifugation (SCU)[24], density gradient centrifugation (DGC), and polymer-based precipitation (PBP) method aka pellet-down method[25]. The SEC method is based on the differential elution profiles of particles of different sizes running through a porous polymer (gel filtration matrix). Small particles such as proteins are slowed down by entering the pores of the polymer's pores while EVs travel quicker along the column and elute first[26,27]. Compared with other methods, SEC could separate different EV subtypes and proteins with minimal effect on EV composition and structure[28]. In the present study, we use the SEC method to separately collect different EV fractions such as large and small EVs and investigate EV markers such as tetraspanins (CD9, CD63) and two homologs of HSP90-α and β derived from macrophages.

Visualization of EVs enables tracking the dissemination of the vesicles in vitro and in vivo. Palmitoylation is the covalent attachment of fatty acids to cysteine (S-palmitoylation) and less frequently to serine and threonine (O-palmitoylation) residues of membrane-associated proteins. The cellular and vesicular membrane can be labeled with palmitoylation signal (Palm)-tagged fluorescent proteins[3,29]. We have developed stable cell lines that express Palm fused with green fluorescent proteins (palmGFP) and with tandem dimer Tomato (palmTomato), which visualize the membrane of the cells and their EVs[20]. The uptake of EVs by recipient cells are also visible and quantitative using the palm fluorescent EV system[3]. However, it has been uncertain how differently monocyte or macrophage-derived EVs are transmitted to cancer cells. Therefore, in the present study, we investigated EVs' transmission efficiencies derived from monocytes and macrophages to oral cancer cells.

Tumor-derived EVs were able to modulate the tumor microenvironment to foster tumorigenesis, tumor progression, and metastasis. The tumor-derived EVs often contain HSPs[19,30]. We have shown that metastatic oral cancer and metastatic prostate cancer secrete the high levels of HSP90-positive EVs and EV-free HSP90 while targeted knockdown of HSP90α, HSP90β, and their cochaperone CDC37 powerfully diminish EV-driven malignancy events and macrophage M2 polarization in oral cancer [17,19,20,31]. At the same time, HSP90-positive TAMs accumulate in the metastatic oral cancer tissues and infiltrate into the tumors[20].

However, macrophage-derived EVs heterogeneity and their cytotoxicity to cancer cells has not been well understood. In the present study, we aimed to (i) separete small

Preprints (www.preprints.org) | NOT PEER-REVIEWED | Posted: 19 April 2021 doi:10.20944/preprints202104.0464.v1

exosomes, large exosomes, and large EVs and to investigate the transmission efficiency and cytotoxic effect of macrophage-derived EVs to oral cancer cells.

2. Materials and Methods

2.1. Cells

HSC-3 (human oral squamous cell carcinoma cell line) and THP-1 (human monocytic leukemia cell line) were obtained from JCRB Cell Bank. HSC-3 were maintained in D-MEM (Wako, Osaka, Japan), and THP-1 were grown in RPMI-1640 (Wako). All medium was supplemented with 10% fetal bovine serum (FBS; Thermo Fisher Scientific, Waltham, MA) and 1% Antibiotic-Antimycotic solution (Sigma-Aldrich, St. Louis, MO). The medium was replaced every 2 days. For macrophage differentiation, THP-1 cells were treated with 20 nM phorbol 12-myristate 13-acetate (PMA) for 24 h or 48 h. Cells were kept in a humidified incubator with 5% CO_2 at 37℃. Cells were counted using Invitrogen™ Countess™ (Thermo Fisher Scientific). Cellular photomicrographs were taken using a Floid cell imaging station (Thermo Fisher Scientific).

2.2. EV fractionation (SEC and PBP)

For extraction of EVs, the size exclusion chromatography (SEC) method and the modified polymer-based precipitation (PBP) method were used as charted. THP-1 cells were seeded at 1×10^6 cells in a 10-cm dish and cultured for 24 h. Cells were then treated with 20 nM PMA for 24 h or untreated. The medium was changed to 4 mL serum-free fresh medium, and the cell culture supernatant was collected at 48 h after the medium changing. The cell culture supernatant was centrifuged at 2,000 × *g* for 30 min at 4℃ to remove detached cells, and then the supernatant was centrifuged at 10,000 × *g* for 30 min at 4℃ to remove cell debris.

Before the SEC method, the supernatant was concentrated to 500 μL using an ultrafiltration filter (Amicon® Ultra-15 Centrifugal Filter Unit (15 mL / 100-kD); Merck Millipore, Burlington, MA) at 5,000 × *g*, 4℃. The pass-through (less than 100-kD) was used as a non-EV fraction. The concentrate (500 μL) was applied on the SEC column (qEV original/70 nm; Izon, Christchurch, New Zealand) following the column equilibration procedure according to the manufacturer's protocol[22]. The sample was eluted by PBS. Twenty fractions of 500 μL solution passed through were collected in order. We divided the fractions into three major parts (fraction 1-6, 7-9 and 10-20), each concentrated 15 times using ultrafiltration devices (Amicon Ultra-0.5 Centrifugal Filter Unit (0.5 ml / 100-kD, Merck).

For the modified PBP method, the supernatant was filtrated with a 0.2 μm syringe filter as described[31]. Then the pass-through was concentrated using an ultrafiltration filter (Amicon® Ultra-15 Centrifugal Filter Unit (15 mL / 100-kD); Merck) at 5,000 × *g*, 4℃. The concentrate was incubated with Total Exosome Isolation Reagent (Thermo Fisher Scientific) at 4℃ overnight and then centrifuged at 10,000 × *g* for 60 min for precipitation of EVs. The pellet was diluted within 100 μL PBS.

Protein concentrations of EV fractions were analyzed using micro BCA protein assay (Thermo Fisher Scientific).

2.3. Particle size distribution

We applied 40 μL of each concentrated fraction to a disposable solvent resistant micro cuvette (ZEN0040, Malvern Panalytical, UK). Particle diameters of the fractions in a range between 0 and 10,000 nm were analyzed in Zetasizer nano ZSP (Malvern Panalytical).

2.4. Transmission electron microscopy

A 400-mesh copper grid coated with formvar/carbon films was hydrophilically treated. The concentrated fraction (10 μL) was placed on Parafilm, and the grid was floated on the fraction and left for 15 min. The sample was negatively stained with 2% uranyl acetate solution for 2 min. EVs on the grid were visualized with 10,000 times magnification with an H-7650 transmission electron microscope (TEM) (Hitachi, Tokyo, Japan) at Central Research Laboratory, Okayama

Preprints (www.preprints.org) | NOT PEER-REVIEWED | Posted: 19 April 2021 doi:10.20944/preprints202104.0464.v1

2.5. Western blotting

EV and non-EV fractions were prepared as described above. We applied 30 μL of each fraction to SDS-PAGE (8-12 %) (protein amount as follows: Fr. 1-6, 1.51 μg; Fr. 7-9, 3.47μg; Fr. 10-20: 58.54 μg; PBP-EVs, 30 μg; non-EV fraction, 30 μg. The proteins in the gel were transferred to PVDF membranes using a wet method. The membranes were blocked in Tris-buffered saline (TBS) containing 0.05% Tween 20 (TBS-T) and 5% Skim Milk (Fujifilm, Tokyo, Japan) for 1 h with shaking at room temperature (RT). Each membrane was incubated overnight with shaking at 4°C with primary antibodies: rabbit anti-actin (1:200, Sigma-Aldrich), rabbit anti-CD9 (1:2,000, Abcam, Cambridge, UK), rabbit anti-CD63 (1:1,000, System Biosciences, Palo Alto, CA), rabbit anti-HSP90α (1:5,000, GeneTex, Irvine, CA) and rabbit anti-HSP90β (1:1,000, GeneTex) antibodies. Afterward, an anti-rabbit IgG secondary antibody conjugated with HRP (1:2,500, Cell Signaling Technologies) was incubated with the membrane for 1 h while shaking at RT. Membranes were washed before and after antibody reactions three times within TBS-T for 10 min at RT on a shaker. Blots were visualized with an ECL Plus Western blotting substrate (Pierce, Rockford, IL).

2.6. Fluorescence-labeling of cells and EVs

The fluorescent EV reporter constructs were kindly gifted from Dr. Charles P. Lai. Briefly, The lentiviral reporter constructs of CSCW-palmitoylation signal-tandem dimer Tomato (palmT) and CSCW-palmitoylation signal-EGFP (palmG) as described[3,20]. PalmG and PalmT sequences were inserted in SCSGW2 lentivector. For virus production, HEK293T cells were transfected with PalmG or PalmT constructs, psPAX2 packaging plasmid, and pMD2.G envelope plasmid using polyethyleneimine (PEI) Max transfection reagent (Polysciences, Warrington, PA). THP-1 or HSC-3 cells were infected using the spinfection method with the viral solution. Infected/transduced stable cells were selected using puromycin. Single clones were isolated by limiting dilution method. The stable cells were designated as THP1/palmG and HSC-3/palmT.

2.7. EV transmission assay

As donor cells, THP-1/palmG cells were seeded at 1×10^6 cells in a 10-cm dish and cultured for 24 h in RPMI-1640 with 10% FBS and then treated with 20 nM PMA for 24 h or untreated. The cells were washed twice with PBS, and then the culture media was replaced with serum-free medium and cultured for a further 2 days. The culture supernatant was collected and centrifuged at 2,000 × *g* for 30 min at 4℃ to remove detached cells and the supernatant were tenfold concentrated with Amicon Ultra-0.5 Centrifugal Filter Unit and used as CM.

For qualitative analysis, fluorescence images were taken using a confocal laser scanning microscopy (CLSM) system (LSM 780 META, Carl Zeiss) as described before[20,32]. Briefly, recipient cells were seeded on a type I collagen-coated coverslip in a 24-well plate at a density of 2.2×10^4 cells per well and cultured for 24 h in D-MEM with 10% FBS. For quantitative analysis, the fluorescence intensity of EV transmission was measured using ArrayScan High Content Screening (HCS) System (Thermo Fisher Scientific) with channel 485/549/bright field as described previously[3,32,33]. Briefly, as recipient cells, HSC-3/palmT were seeded 5,000 cells per well in a 96-well NanoCulture Plate (NCP) (Medical & Biological Laboratories, Nagoya, Japan) and cultured for 24 h in 200 μL mTeSR1. CM was applied in a ratio 1:1 with a fresh culture medium.

2.8. Cell viability

Cell viability was measured as described previously[34]. ATP content was quantified using CellTiterGlo (CTG) Luminescent Cell Viability Assay (Promega, Madison, WI). To examine the effects of CM, whole EV, and co-culture, HSC-3 cells were seeded at 2×10^4 cells per well in a 24-well plate. After 24 h of culturing, 1) CM: equal volume CM was added to the culture medium, 2) Co-culture: a culture insert with a 0.45-μm pore (Greiner, Kremsmunster, AU) was placed, and THP-1 cells (2×10^4 cells/well) were seeded in the culture insert, 3) EV protein: the whole EV fraction (1.25 μg /ml) prepared using the SEC or PBP method was added. After culturing for another 48 h, cells were detached using

Preprints (www.preprints.org) | NOT PEER-REVIEWED | Posted: 19 April 2021 doi:10.20944/preprints202104.0464.v1

Trypsin/EDTA and suspended with 150 μL CTG solution and then incubated for 10 min at 37℃. Luminescence was measured using the plate reader Gemini XP SOK (Molecular Devices).

To examine the effects of EV fractions separated using the SEC method, HSC-3 cells (5,000 cells /well/ 200 μL) were seeded to a 96-wells plate. After 24 h of culturing, 10 μL of EV fractions (Fr. 1-6, 7-9, or 10-20) were added to each well (quadruplicate). After culturing for another 48 h, 150 μL medium was removed from each well and 50 μL CTG solution was added. Luminescence was measured on the Gemini XP SOK.

2.9. Flow cytometry

Phycoerythrin (PE)-conjugated mouse monoclonal anti-human antibodies were used for cell surface staining: anti-CD14, anti-CD80, anti-CD206 and anti-CD68 antibodies (all from BioLegend, San Diego, CA). Isotype-matched negative controls (CD14, mouse IgG2aκ; CD68, mouse IgG2bκ; CD80 and CD206, mouse IgG1κ) were used throughout the investigations. THP-1 cells and PMA-induced macrophages were cultured in a serum-free medium for 48 h. PMA-induced macrophages were unattached with Accutase (Innovative Cell Technologies, San Diego, CA) and centrifuged at 200 × *g* for 5 min at 4℃. The pellet was washed with PBS containing 0.5% bovine serum albumin (BSA, Wako). Fc receptors were blocked by incubating the cells with 25 μg/ml Fc receptor blocking solution (Human TruStain FcX™, BioLegend) for 10 min at RT before antibody staining. To detect cell surface markers, 5 μL of monoclonal mouse anti-human antibodies or the relevant isotypes were incubated with samples for 30 min at 4℃. For intracellular staining (CD68), cells were fixed with 4% paraformaldehyde (PFA) phosphate buffer solution (Wako) and permeabilized with Nonidet P-40 (NP-40; Sigma-Aldrich). The stained cells were analyzed using a MACSQunat®X flow cytometer (Miltenyi Biotec, Bergisch Gladbach, DE), and more than 4,000 events were measured per sample. The flowcytometric analyses were carried out using MACSQunat2.6 software (Miltenyi Biotec). All experiments were performed in triplicate.

2.10. Statistical Analysis

Statistical significance was calculated using GraphPad Prism and Microsoft Excel. The difference between the two sets of data was examined by unpaired student's t-test. $P < 0.05$ was considered to indicate statistical significance. Data were expressed as means ± SD unless otherwise specified.

2. Results

2.1. Differentiation of monocytic cells into macrophages

We first examined whether PMA stimulation on THP-1 monocytic cells could foster macrophage differentiation into M0, M1, or M2-types. For this purpose, we examined the size and shapes of non-treated THP-1 and PMA-stimulated THP-1. The cells were attached to the culture dish and enlarged after PMA stimulation (Figure 1 A, B). Flow cytometry showed that the cells with PMA stimulation showed a higher percentage in the larger size (vertical axis; FSC) and higher internal complexity such as granularity (horizontal axis; SSC) than non-treated cells (Figure 1C).

Preprints (www.preprints.org) | NOT PEER-REVIEWED | Posted: 19 April 2021 doi:10.20944/preprints202104.0464.v1

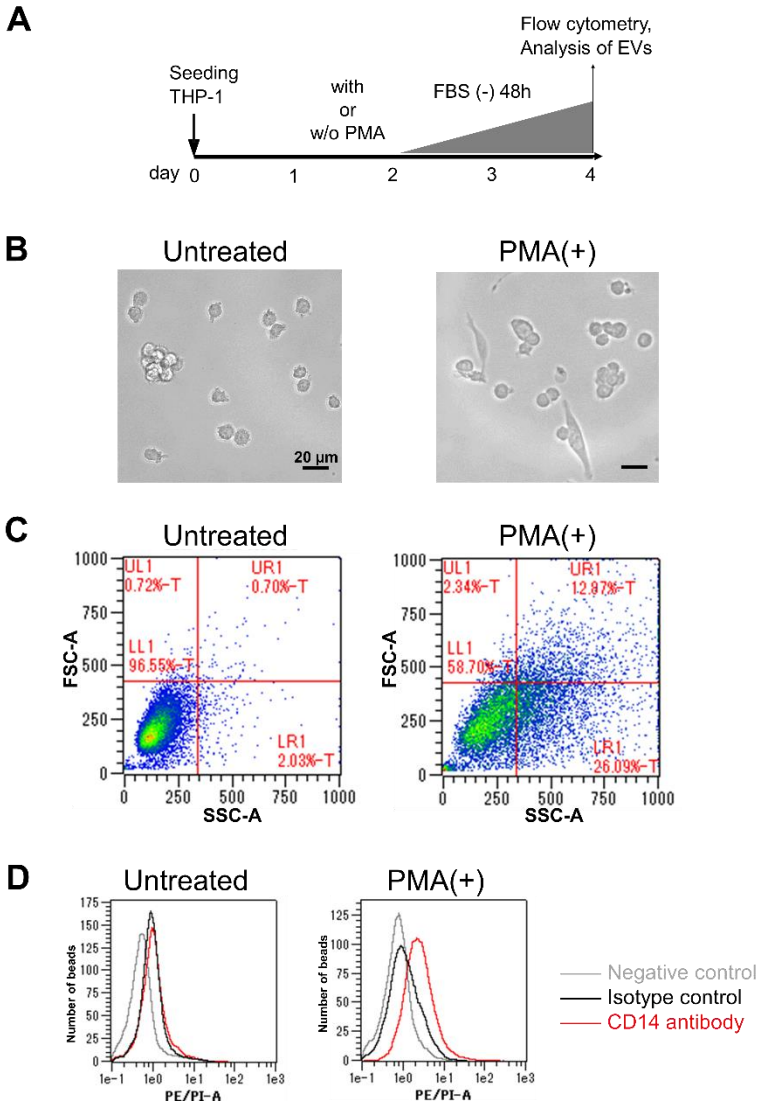

Figure 1. Differentiation of monocytic cells stimulated with PMA into macrophages. (A) A scheme of experimental protocols. THP-1 cells were stimulated with PMA for 24 h or unstimulated. (B) Representative images of PMA-treated and non-treated THP-1 cells. Scale bars, 20 μm. (C) Size (FSC) and complexity (SSC) of PMA-treated and non-treated THP-1 cells were determined by flow cytometry. (D) Flow cytometry detecting cell surface CD14 on macrophages (PMA-treated THP-1) but not on untreated THP-1 cells. Data are representative of three independent experiments. See supplemental figure S1 for M1 and M2 markers.

To determine the subtypes of these cells, we next examined the expression of CD14, CD68, CD80 and CD 206 in the untreated vs. PMA-stimulated THP-1 cells. The expression of CD14 was markedly increased in PMA-stimulated THP-1 cells (Figure 1D), indicating that the THP-1 cells were differentiated into the macrophage lineage. Meanwhile, intracellular and cell-surface CD68 (markers of pan-macrophages), CD80 (a marker of M1 macrophages), and CD206 (a marker of M2 macrophages) did not differ compared to their isotype controls (Figure S1).

These data indicate that PMA-stimulated THP-1 monocytic cells were differentiated into macrophages but neither M1 nor M2 types.

2.2. High transmission efficiency of macrophage-derived EVs to oral cancer cells

To monitor macrophage-derived EVs' uptake by oral cancer cells, we labeled the membrane of THP-1 cells and their EVs with palmGFP and of HSC-3 cells with Palm-

Preprints (www.preprints.org) | NOT PEER-REVIEWED | Posted: 19 April 2021 doi:10.20944/preprints202104.0464.v1

Tomato. Then, we confirmed that the palm-fluorescent proteins were successfully expressed in these cells (Figure 2A). Besides, THP-1/palmG cells were differentiated by stimulating with PMA to macrophage/palmG, which were more attaching to the dishes and larger shapes (Figure 2A, arrows).

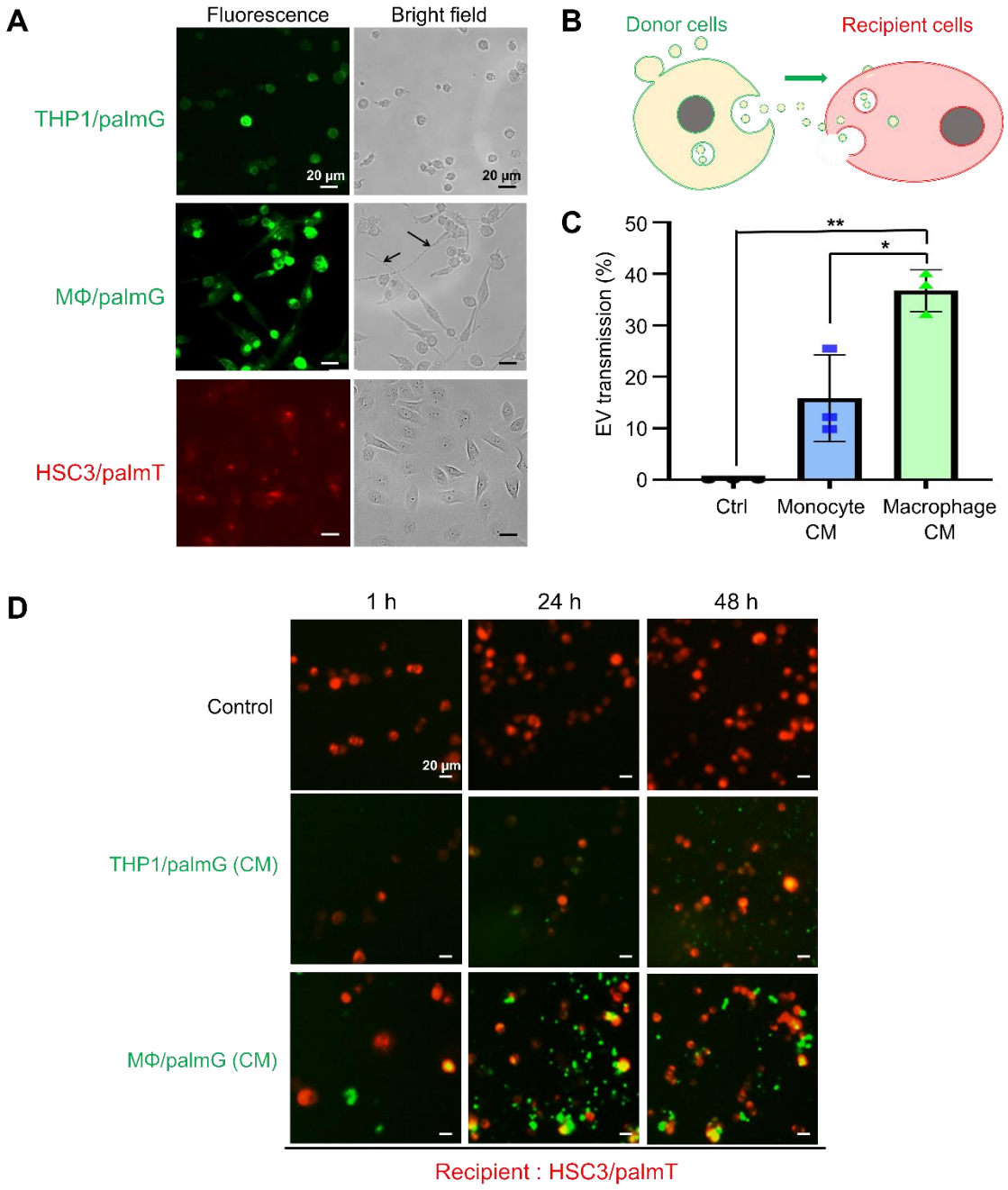

Figure 2. A higher transmission efficiency of macrophage-derived fluorescent EVs than monocyte-EVs to oral cancer cells. Palmitoylation signal-fused with enhanced GFP (palmG) (shown as green) and with tdTomato (palmT) (shown as red) were stably expressed in THP-1 or HSC-3 cells, respectively, and designated as THP1/palmG and HSC3/palmT. The THP1/palmG was stimulated with PMA for macrophage differentiation. (A) Representative images of THP1/palmG, MΦ/palmG and HSC3/palmT cells. (B) A schema of the concept for the analysis of EV transfer. (C) Transmission efficiencies of EVs at 24 hours after the addition. n=3, *P<0.05, **P<0.01 (D) Representative images of EV transfer. The recipient HSC3/palmT cells (red) cultured in NanoCulture Plate (NCP) were treated with the serum-free RPMI-1640 (control) or conditioned medium (CM) of MΦ/palmG and THP1/palmG. Images were taken at 0, 24, 48 hours after the addition.

Preprints (www.preprints.org) | NOT PEER-REVIEWED | Posted: 19 April 2021 doi:10.20944/preprints202104.0464.v1

Next, we confirmed the transmission of macrophage-derived EVs to macropahges themselves (Figure S2A) and to oral cancer cells in 2D culture (Figure S2B). Then, we examined the transmission efficiency of the fluorescent EVs into oral cancer cells in a 3D culture environment. The macrophage-EVs' transmission efficiency to the oral cancer cells was significantly higher than that of monocytes (Figure 2 B, C, D). The monocyte-EVs were transmitted to 15.8 % of the recipient HSC-3 cells while macrophage EVs to 36.7% of the recipient cells (Figure 2C).

These data indicate that macrophage-derived EVs were highly transmissive to oral cancer cells compared with monocyte-derived EVs.

2.3. The cytotoxicity of unidentified macrophage-secreted factor to oral cancer cells

To examine whether macrophage-secreted factors were cytotoxic to cancer cells, we next established intercellular communication experiments using conditioned medium (CM) and transwell-based co-culture system (Figure 3A). Then, we examined the cell viability of the HSC-3 cells after receiving macrophage-derived CM or in the co-culture system. The CM of macrophages reduced ATP activity of HSC-3 cells (Figure 3B), whereas the CM of monocytes increased the ATP activity. ATP activity of HSC-3 cells after co-culturing with macrophages was reduced to 65% (Figure 3C), whereas co-culturing with monocytes did not alter the ATP activity.

These data suggest that macrophages released cytotoxic factors to oral cancer cells.

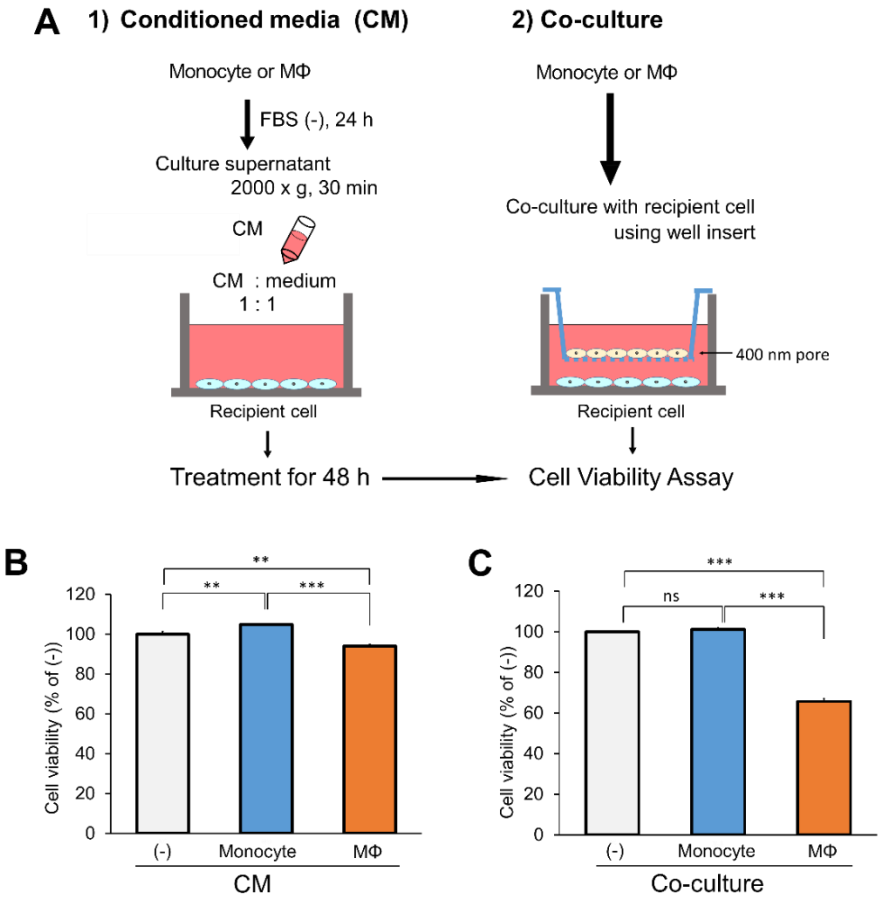

Figure 3. Cytotoxicity of macrophage-EVs to oral cancer cells. (A) Schemas of experimental designs. (1) HSC3/palmT cells were treated with CM collected from THP1/palmG or MΦ/palmG for 48 h. (2) THP1/palmG or MΦ/palmG cells were co-cultured with HSC3/palmT cells using well insert (400 nm pore) for 48 h. (B) Cell viability of HSC3/palmT cells treated with CM. (C) Cell viability of HSC3/palmT cells co-cultured with the THP1/palmG or MΦ/palmG. N=3, *P<0.05, **P<0.01 and ***P<0.001.

Preprints (www.preprints.org) | NOT PEER-REVIEWED | Posted: 19 April 2021 doi:10.20944/preprints202104.0464.v1

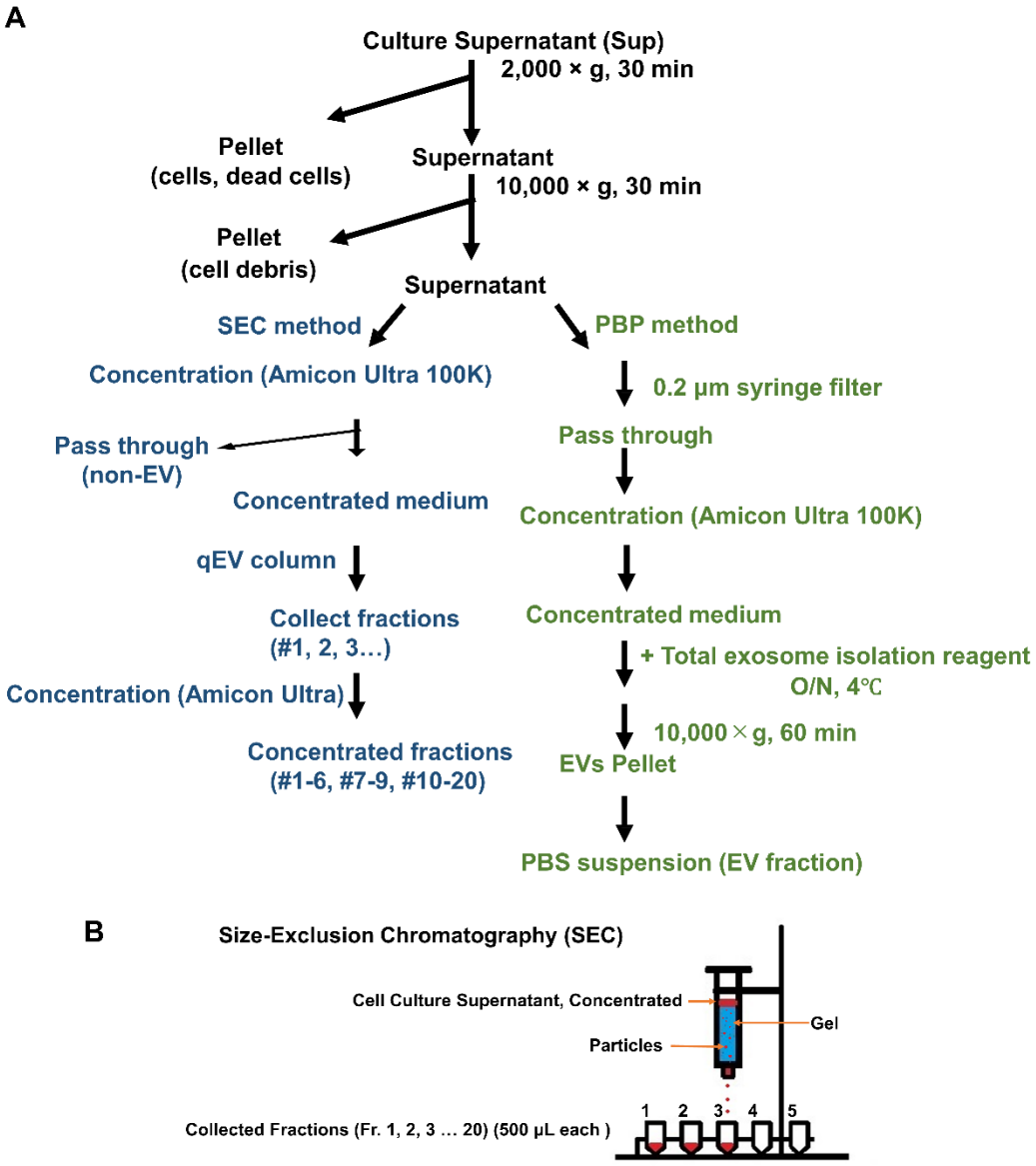

Figure 4. SEC method and PBP method for EV preparation. (A) A flow chart of the SEC method and PBP method. (B) A scheme of the SEC method.

2.4. Separation of small exosomes, large exosomes, and large EVs

The heterogeneity of EVs with different marker proteins could lead to a diversity in EV's functions[35]. To ask how different EV types were isolated by different methods, we next used the SEC method and PBP method (Figure 4A). Using the SEC method, we first separated the culture supernatant into 20 fractions (Fraction 1, 2, 3…20) (Figure 4B). To simplify the EV analysis, we gathered these fractions into three: Fraction 1-6 (Fr. 1-6), Fraction 7-9 (Fr. 7-9), and Fraction 10-20 (Fr. 10-20) (Figure S3).

The cup-like shapes were found in macrophage-derived and monocyte-derived EVs by TEM, indicating both cell types secreted exosomes (Figure 5 A-E). Macrophage-EVs' size appeared to be larger and more various than monocyte-EVs (Figure 5 A, B). In the Fr. 1-6, a few "large EVs" with the size of approximately 200 nm were observed by TEM (Figure 5C). In the Fr. 7-9, small EVs (50-100 nm) were observed under TEM (Figure 5D). These small EVs were suggested as large exosomes (EXO-L) from the size. In the fraction 10-20, few EVs (approximately 30 nm) and a high density of proteins were visible in the field of

 doi:10.20944/preprints202104.0464.v1

TEM (Figure 5E), suggesting that the Fr. 10-20 could contain small exosomes (EXO-S) and vesicle-free proteins.

Next, the particle diameter distribution analysis revealed that the size of monocyte-EVs was peaked at 165.8 nm in the range between 50-500 nm, while that of macrophage-EVs was peaked at 205.1 nm in the wider range between 50-1000 nm (Figure 5 F, G), suggesting that macrophage-EVs' size was larger and more various than monocyte-EVs.

In the Fr. 1-6 of the SEC method, the particle size was between 100-500 nm peaked at 208.9 nm (Figure 5H), suggesting that the Fr. 1-6 contained large EVs (larger than exosomes). In the Fr. 7-9, particle size was ranged between 50-300 nm with a peaked size of approximately 150 nm (Figure 5I), suggested as large exosomes (EXO-L) from the size. In the fraction 10-20, the particles' size was smaller than 100 nm and peaked at approximately 40 nm (Figure 5J), consist with the TEM. Thus, the Fr. 10-20 could contain small exosomes (EXO-S) and vesicle-free proteins.

To characterize the small and large exosomes or larger EVs by protein markers, we next performed western blotting of tetraspanins (CD9, CD63: established EV markers), HSP90α, HSP90β, and β-actin. CD9 was markedly detected in the EXO-L fraction (Fr. 7-9) (Figure 5K, L; Figure S4, S5). On the other hands, CD63, another tetraspanin family member often found in EVs, was markedly detected in the Fr. 10-20 (EXO-S and free proteins) while degradation of CD63 was seen in the Fr. 7-9 (Figure S5), suggesting that CD63 might be selectively cleaved out from the EXO-S by metalloproteinases[3,32]. HSP90α, HSP90β and β-actin were markedly found in the Fr. 10-20 (Figure 5 K, L), suggesting that these HSP90 homologs and β-actin mainly existed in EXO-S and/or as vesicle-free forms. Additionally HSP90β was detectable in the EXO-L fraction (Fr. 7-9) as well, while not contained in the large EV fraction.

These data indicate that different types of EVs can be separately isolated using the SEC method as EXO-L, EXO-S and large EVs. These data also suggest that macrophages released CD9-positive large exosomes (EXO-L), CD63/HSP90α/HSP90β-positive small exosomes.

Preprints (www.preprints.org) | NOT PEER-REVIEWED | Posted: 19 April 2021 doi:10.20944/preprints202104.0464.v1

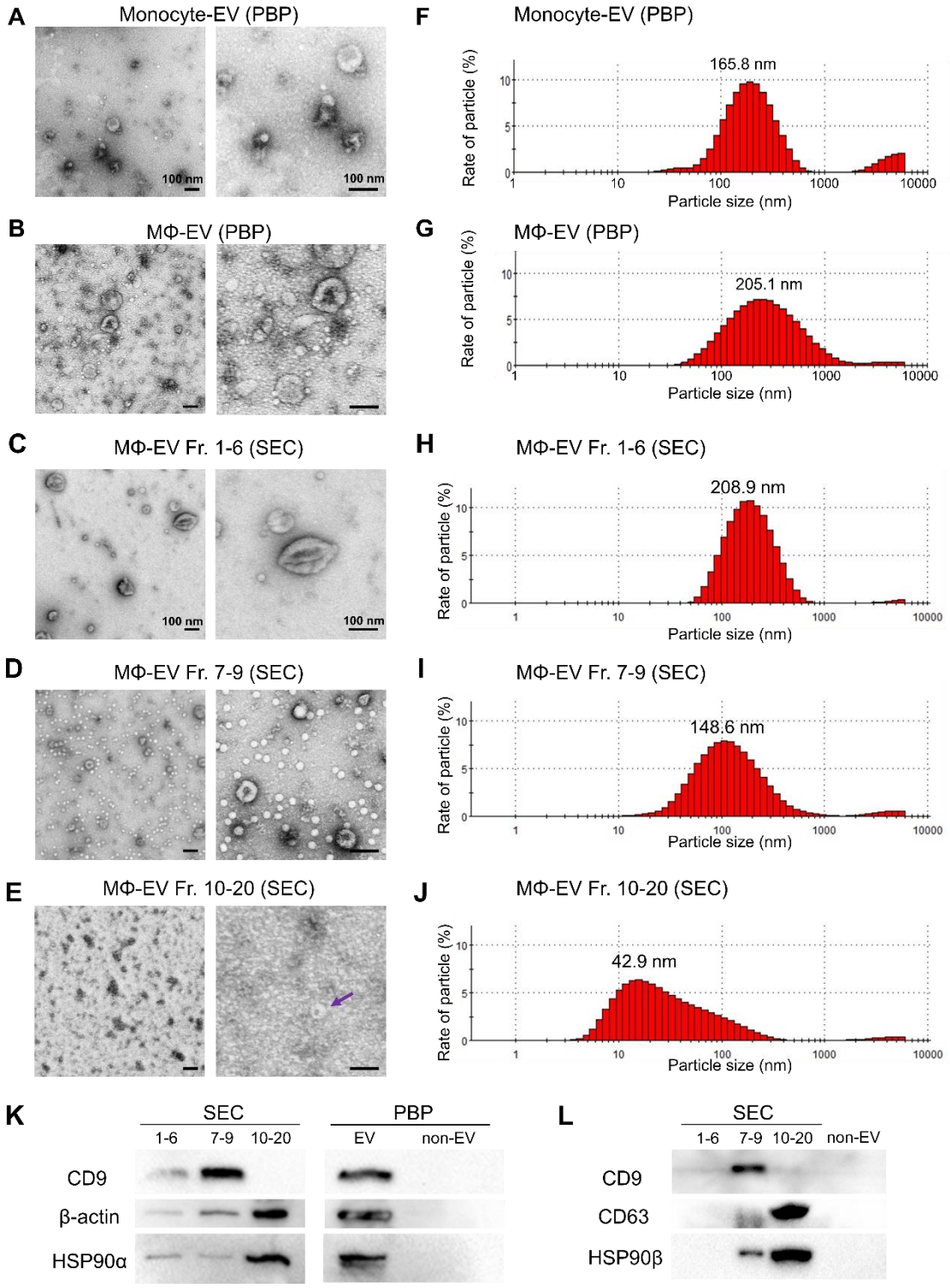

Figure 5. Characterization of small exosomes, large exosomes and large EVs prepared by using size exclusion chromatography (SEC) method. Conditioned medium was collected from (A) untreated or (B-E) PMA-treated THP-1 cells at 48 h after changing into serum-free medium. (C-E) In the SEC method, twenty fractions were first collected and then concentrated into three fractions (Fr.1-6, Fr.7-9, and Fr.10-20). Details were shown in Figure S3. (A-E) Representative TEM images of EVs derived from (A) monocytic cells and (B-E) macrophages. Scale bars, 100 nm. (F-J) Particle diameter distribution of the EV fractions. (K) Western blotting of CD9, HSP90α and β-actin. (L) Western blotting of CD9, CD63, and HSP90β.

2.5. The cytotoxicity of macrophage-derived fraction 10-20 (small exosomes and free proteins) to oral cancer cells

Preprints (www.preprints.org) | NOT PEER-REVIEWED | Posted: 19 April 2021 doi:10.20944/preprints202104.0464.v1

To examine EVs' cytotoxicity derived from macrophages on oral cancer cells, we stimulated the HSC-3 cells with fractions (Fr. 1-6, 7-9, and 10-20) and then measured ATP activity. The morphology of HSC-3 cells was changed to spindle-like shapes after applying the Fr. 10-20 (EXO-S and free proteins) but not by the Fr.1-6 nor the Fr.7-9 (Figure 6A). The Fr. 10-20 tended to lower the viability of HSC-3 cells (P=0.0863), which was more effective than the other two fractions (Figure 6B).

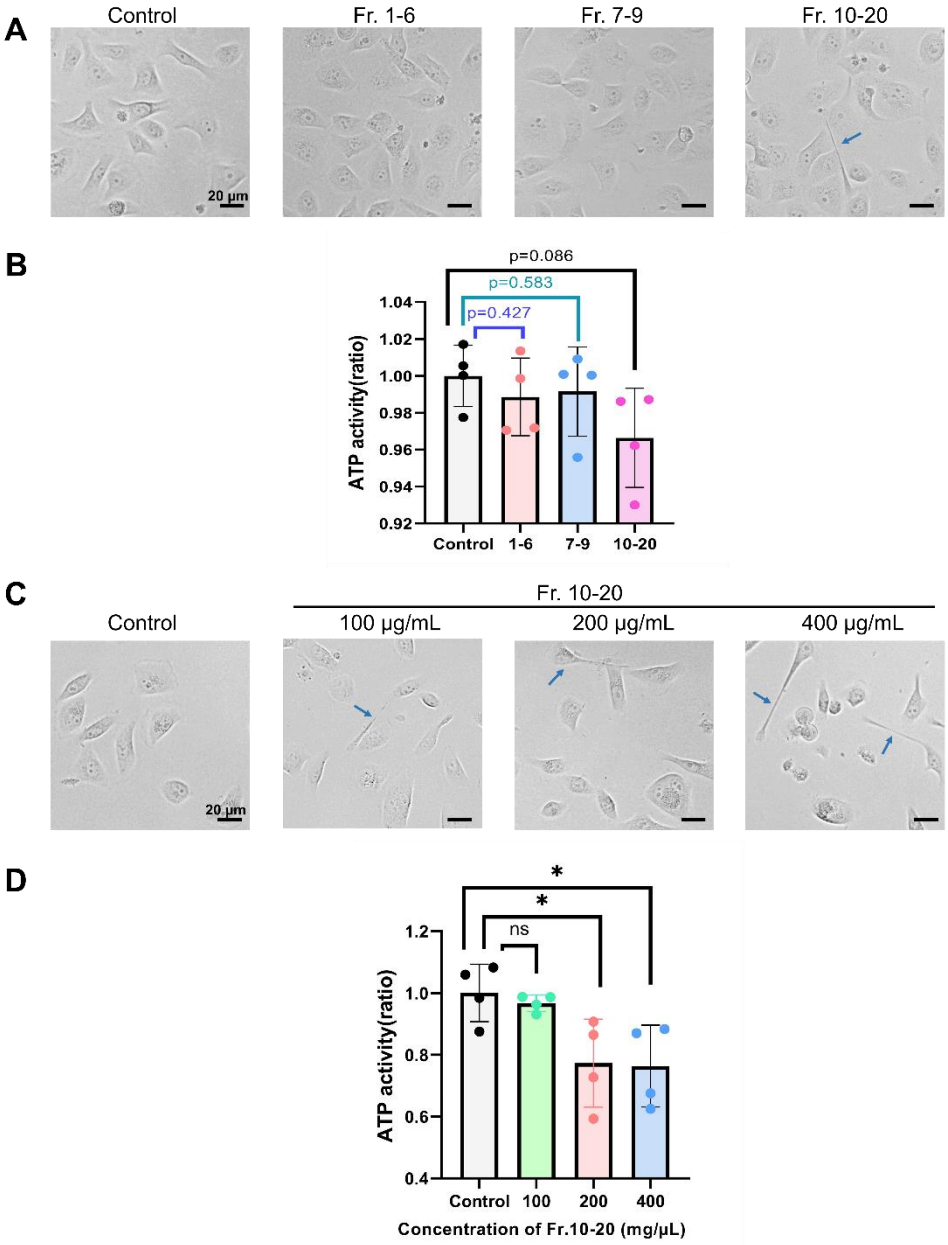

Figure 6. Cytotoxicity of macrophage-derived small exosomes to oral cancer cells. EV fractions were prepared from macrophages by the SEC method and administrated to HSC-3 cells for 48 hours. ATP activity was measured to determine the cytotoxicity. (A) Representative images of HSC-3 cells treated with the fractions (10 μL each) for 48 hours. Scale bars, 20 μm. Arrows: spindle shape cells. (B) Relative ATP activity of the recipient HSC-3 cells treated with the fractions. N=4. (C, D) Cell viability after applying different concentrations of Fr. 10-20. (C) Representative images of HSC-3 treated with Fr. 10-20 at the final concentrations of 100, 200, or 400 μg/mL for 48 hours. PBS (40 μL) was added to control groups. Scale bars, 20 μm. (D) Relative ATP activity of HSC-3 cells treated with Fr. 10-20 in the different concentrations to HSC-3 cells. The figure was shown as a ratio to control groups. N=4. *P<0.05. n.s., not significant.

We next examined the effects of three different concentrations (100 μg/mL, 200 μg/mL, and 400 μg/mL) of the Fr. 10-20 on the oral cancer cells. The spindle shapes were

Preprints (www.preprints.org) | NOT PEER-REVIEWED | Posted: 19 April 2021 doi:10.20944/preprints202104.0464.v1

found in the HSC-3 cells stimulated with these fractions, whereas not found in the unstimulated cells (Figure 6C). Simultaneously, the cell viability of HSC-3 cells was reduced to approximately 77% after applying the higher concentration (200 μg/mL and 400 μg/mL) of the Fr. 10-20 (Figure 6D).

These data indicate that macrophages-derived EXO-S could be cytotoxic to oral cancer cells.

3. Discussion

The heterogeneity of EVs and extracellular particles is recently a crucial issue in biology and medicine. Many methodologies have been developed to separate various EVs according to the surface marker specificity, EV size, and density. The SEC method enables the separation of vesicle and protein fractions according to their size. Indeed, we first collected twenty fractions from macrophage CM and then finally analyzed three fractions, including the large EV fraction (Fr. 1-6, with CD9, HSP90α, and β-actin), EXO-L fraction (Fr. 7-9, with CD9, HSP90, β-actin), and EXO-S with vesicle-free proteins (Fr. 10-20, containing CD63, HSP90, and β-actin). Our data suggest that macrophage-derived anti-cancer cytotoxic factors could be contained in EXO-S or exist in vesicle-free form (Figure 7).

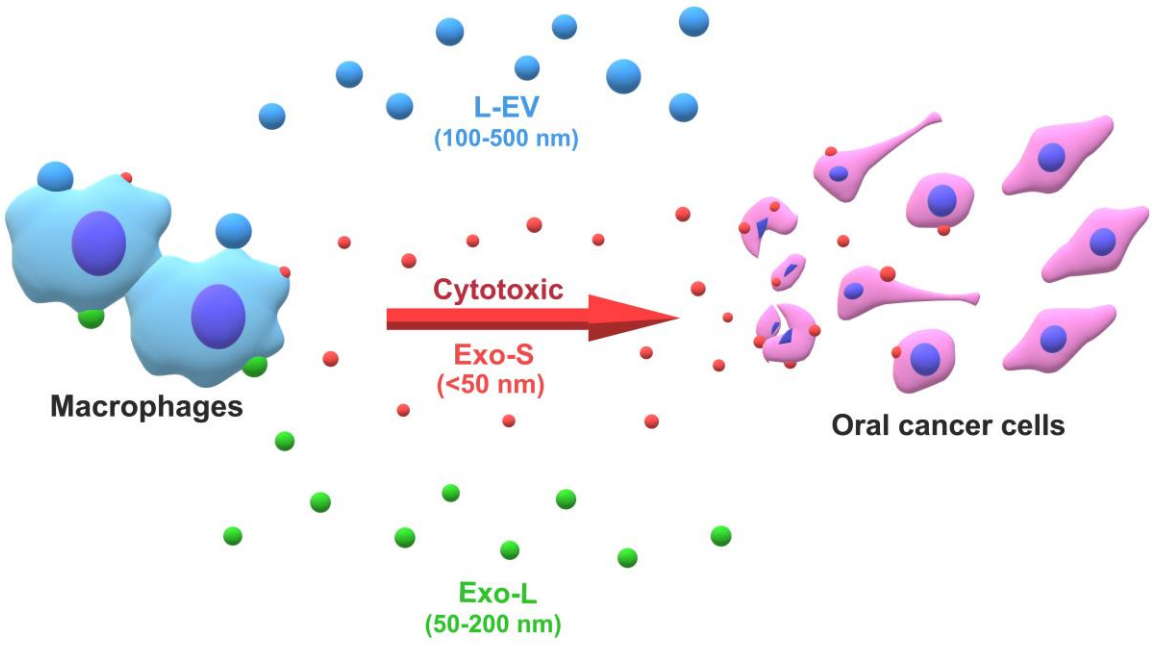

Figure 7. Graphical abstract. Macrophage-derived small exosomes (EXO-S) prepared by SEC method showed cytotoxicity to oral cancer cells. EXO-S was rich in CD63, HSP90α and HSP90β. Large EVs (L-EVs) and CD9/HSP90β-positive large exosomes (EXO-L) were not cytotoxic.

Protein markers of EVs had been well investigated by many researchers and organized in MISEV2018[16]. However, some proteins such as HSP90, β-actin, and even tetraspanins have been detected in many fractions, including large and small exosomes, large and small EVs, and vesicle-free protein fractions in the context-dependent manner[17,19,20]. We previously found that EVs prepared by a modified PBP method contained marked concentrations of CD9, β-actin, and HSP90 than those from the ultracentrifugation method[36]. Reproducibly, CD9, and HSP90α were markedly detected in macrophage-derived EVs isolated by the PBP methods in the present study. However, it has been noticed that the precipitating agents may interfere with the structures in EVs, whereas SEC was proved to minimally affect EV composition[28]. In the SEC method,

isolation of vesicles from plasma or serum often caused co-isolation of high-density lipoprotein (HDL)[37]. Besides, low-density lipoprotein (LDL) can bind onto the isolated EVs. These characteristics often resulted in lipoproteins contamination in EVs[38].

Consequently, it was difficult to separate lipoproteins with EVs by SEC[23,39]. The key members of the tetraspanin family, CD9 and CD63, were usually used as exosomes markers, whereas they were also detectable in other types of EVs[40]. EVs consisted of heterogeneous subtypes, among which CD9 was mainly contained in Exo-L (90-120 nm), while CD63 was in Exo-S (60-80 nm)[7]. The distinction of EV markers can be explained by their origin because CD9-positive EVs are formed at the plasma membrane and early endocytic locations, while CD63-positive EVs were specifically abundant in proteins associated with endosomes, multivesicular bodies (MVB), vacuoles, and phagocytic vesicles[7,40]. In the present study, Exo-L with a strong CD9 signal was mainly presented in faction 7-9, while Exo-S appeared to be presented only in the fraction 10-20. Moreover, HSP90 showed a stronger signal in the fraction 10-20 (containing EXO-S and free proteins) than in fraction 7-9 (EXO-L). HSP90 plays key roles in phagocytosis and antigen cross-presentation of antigen-presenting cells (APC) such as dendritic cells and macrophages [30,41,42]. Also, cancer cells often release HSP90-rich EVs and vesicle-free HSP90, which are targetable for cancer therapy [19,20,43]. Indeed, HSP90-rich tumor-infiltrating macrophages were detected in oral cancer specimens of patients[20]. The targeted knockdown of HSP90 in oral cancer cells significantly reduced exosome release and transmission efficiency to macrophages[20]. Thus, both cancer cells and TAMs express HSP90 that involves vesicle uptake, phagocytosis, and antigen presentation. Our findings of HSP90α and HSP90β in the macrophage-derived exosomes and as vesicle-free proteins are vital for further studies on the roles of HSP90 in macrophage polarization and the effect of macrophage-derived EVs on cancer cells.

Cancer cells are often sensitive to extracellular microenvironment and signals. We previously showed that cell stress could induce cell morphology changes such as increasing round and spindle-shaped cells, and these morphological changes involve epithelial-to-mesenchymal transition (EMT)[19,42]. A similar morphological variation was observed in the present study after treating the oral cancer cells with the fraction 10-20 (containing EXO-S and free proteins) (Figure 5). It has been shown that Exo-S, exomeres[7], and other types of proteins generally were contained in the Fr. 10-20 obtained by the SEC method. Comparing to the other EV fractions, the cytotoxicity in the CM and EXO-S might have been caused by cytokines such as interferon-γ (IFN-γ)[44], tumor necrosis factor α (TNF-α), and effector molecules such as nitric oxide (NO) secreted by macrophages. HSPs are molecular chaperones that assist functional protein folding, presumably of cytotoxic factors [42,45,46]. Although our current study identified the transmission of macrophage-EVs and the characteristic of different EV fractions, it is still unclear what kind of factors in the CM was cytotoxic to the cancer cells.

Nonetheless, apart from cytokines, it has been shown that macrophage-derived EVs involved anti-tumor activity. For instance, macrophages exposed to environmental stresses, such as nutrient deprivation, hypoxia, and the signaling factors released from cancer cells could recruit diverse intracellular factors and package them into secretory vesicles to mediate the primary response against cancer cells until the immune surveillance system was activated[47]. It was also found that macrophages cultured in glucose-depleted medium secreted human glycyl-tRNA synthetase 1 (GARS1)-EVs, which involved immunological defense response against tumorigenesis and could promote cancer cell death[47,48]. Relevantly, we emphasize the powerful transmission ability of macrophage-derived EVs. The EV isolation method shown in the present study indicates macrophage-derived EVs' potential roles in targeted therapeutics against tumors.

5. Conclusions

In conclusion, using a fluorescent EV reporter system, we monitored that macrophage-derived EVs were highly transmissive to cancer cells. Our data indicate that macrophages release cytotoxic factors on oral cancer cells. The cytotoxic vesicle-free fraction

was rich in CD63 and HSP90. Additionally, different types of EVs such as S-EVs and L-EVs were separated using the size-exclusion chromatography from the vesicle-free proteins.

Supplementary Materials: The following are available online at www.mdpi.com/xxx/s1, Figure S1: flow cytometry of CD14, CD68, CD80, and CD206 in PMA-treated and untreated THP-1 cells, Figure S2: confocal microscopy of the transmission of macrophage-derived fluorescent EVs, Figure S3: preparation of Fr. 1-6, Fr. 7-9, and Fr. 10-20 from the SEC method, Figure S4: full images of western blot analysis shown in Figure 4H, Figure S5: full images of western blot analysis shown in Figure 4I.

Author Contributions: Conceptualization, T.E. and C.S.; methodology, C.S., Y.L. and T.E.; software, Y.L., C.S. and T.E. ; validation, Y.L., C.S. and T.N.; formal analysis, Y.L. and C.S.; investigation, Y.L., C.S., T.N., E.A.T., M.T.T., P.W., and S.F.; resources, T.E. and K.O.; data curation, Y.L., T.E. and C.S.; writing—original draft preparation, Y.L. and T.E.; writing—review and editing, T.E., C.S. and K.O.; visualization, Y.L., T.E., T.N. and C.S.; supervision, T.E., C.S., T.M. and K.O.; project administration, T.E. and C.S.; funding acquisition, T.E., C.S., T.M. and K.O. All authors have read and agreed to the published version of the manuscript.

Funding: This research was funded by Suzuken Memorial Foundation (T.E.), JSPS Kakenhi, grant number 17K11642 (T.E.), 17K11669-KOh (T.E., C.S.), 20K09904 (C.S., T.E., K.O.), 19H03817-MT (T.E.), 20H03888- HN (T.E.), 20K20611-MT (T.E.), and Ryobi Teien Memorial Foundation (T.E., C.S., K.O.)

Acknowledgments: The authors thank Hitoshi Higuchi, Shigeru Maeda, Eriko Aoyama, Yuka Okusha, Mami Fujiwara, Yukiko Nishioka, Mai Nakanou, Akiko Kawase, Yuka Wakasugi, Kazuko Kobayashi and Eiji Matsuura for their cooperation, mentorship, and/or support. We thank Noa Matsuda, Kaho Noda, Kanna Yamasaki, and Hideki Namba for useful discussion.

Conflicts of Interest: The authors declare no conflict of interest.

References

1. Colombo, M.; Raposo, G.; Théry, C. Biogenesis, secretion, and intercellular interactions of exosomes and other extracellular vesicles. *Annu. Rev. Cell Dev. Biol.* **2014**, *30*, 255–289, doi:10.1146/annurev-cellbio-101512-122326.
2. Yáñez-Mó, M.; Siljander, P.R.-M.; Andreu, Z.; Bedina Zavec, A.; Borràs, F.E.; Buzas, E.I.; Buzas, K.; Casal, E.; Cappello, F.; Carvalho, J.; et al. Biological properties of extracellular vesicles and their physiological functions. *J. Extracell. Vesicles* **2015**, *4*, 27066, doi:10.3402/jev.v4.27066.
3. Taha, E.A.; Sogawa, C.; Okusha, Y.; Kawai, H.; Oo, M.W.; Elseoudi, A.; Lu, Y.; Nagatsuka, H.; Kubota, S.; Satoh, A.; et al. Knockout of MMP3 weakens solid tumor organoids and cancer extracellular vesicles. *Cancers (Basel).* **2020**, *12*, 1–29, doi:10.3390/cancers12051260.
4. El Andaloussi, S.; Mäger, I.; Breakefield, X.O.; Wood, M.J.A. Extracellular vesicles: Biology and emerging therapeutic opportunities. *Nat. Rev. Drug Discov.* **2013**, *12*, 347–357, doi:10.1038/nrd3978.
5. Lawson, C.; Vicencio, J.M.; Yellon, D.M.; Davidson, S.M. Microvesicles and exosomes: new players in metabolic and cardiovascular disease. *J. Endocrinol. 228*, R57–R71, doi:10.1530/JOE-15-0201.
6. Battistelli, M.; Falcieri, E. Apoptotic bodies: Particular extracellular vesicles involved in intercellular communication. *Biology (Basel).* **2020**, *9*, doi:10.3390/biology9010021.
7. Zhang, H.; Freitas, D.; Kim, H.S.; Fabijanic, K.; Li, Z.; Chen, H.; Mark, M.T.; Molina, H.; Martin, A.B.; Bojmar, L.; et al. Identification of distinct nanoparticles and subsets of extracellular vesicles by asymmetric flow field-flow fractionation. *Nat. Cell Biol.* **2018**, *20*, 332–343, doi:10.1038/s41556-018-0040-4.
8. Meehan, B.; Rak, J.; Di Vizio, D. Oncosomes - large and small: what are they, where they came from? *J. Extracell. vesicles* **2016**, *5*, 33109, doi:10.3402/jev.v5.33109.

9. Vagner, T.; Spinelli, C.; Minciacchi, V.R.; Balaj, L.; Zandian, M.; Conley, A.; Zijlstra, A.; Freeman, M.R.; Demichelis, F.; De, S.; et al. Large extracellular vesicles carry most of the tumour DNA circulating in prostate cancer patient plasma. *J. Extracell. Vesicles* **2018**, *7*, doi:10.1080/20013078.2018.1505403.
10. Chen, Q.; Bei, J.J.; Liu, C.; Feng, S. Bin; Zhao, W.B.; Zhou, Z.; Yu, Z.P.; Du, X.J.; Hu, H.Y. HMGB1 induces secretion of matrix vesicles by macrophages to enhance ectopic mineralization. *PLoS One* **2016**, *11*, 1–18, doi:10.1371/journal.pone.0156686.
11. Mebarek, S.; Abousalham, A.; Magne, D.; Do, L.D.; Bandorowicz-Pikula, J.; Pikula, S.; Buchet, R. Phospholipases of mineralization competent cells and matrix vesicles: roles in physiological and pathological mineralizations. *Int. J. Mol. Sci.* **2013**, *14*, 5036–5129, doi:10.3390/ijms14035036.
12. Huang, Y.; Zucker, B.; Zhang, S.; Elias, S.; Zhu, Y.; Chen, H.; Ding, T.; Li, Y.; Sun, Y.; Lou, J.; et al. Migrasome formation is mediated by assembly of micron-scale tetraspanin macrodomains. *Nat. Cell Biol.* **2019**, *21*, 991–1002, doi:10.1038/s41556-019-0367-5.
13. Raposo, G.; Stoorvogel, W. Extracellular vesicles: exosomes, microvesicles, and friends. *J. Cell Biol.* **2013**, *200*, 373–383, doi:10.1083/jcb.201211138.
14. Seyama, M.; Yoshida, K.; Yoshida, K.; Fujiwara, N.; Ono, K.; Eguchi, T.; Kawai, H.; Guo, J.; Weng, Y.; Haoze, Y.; et al. Outer membrane vesicles of Porphyromonas gingivalis attenuate insulin sensitivity by delivering gingipains to the liver. *Biochim. Biophys. Acta - Mol. Basis Dis.* **2020**, *1866*, 165731, doi:https://doi.org/10.1016/j.bbadis.2020.165731.
15. Kim, O.Y.; Park, H.T.; Dinh, N.T.H.; Choi, S.J.; Lee, J.; Kim, J.H.; Lee, S.-W.; Gho, Y.S. Bacterial outer membrane vesicles suppress tumor by interferon-γ-mediated antitumor response. *Nat. Commun.* **2017**, *8*, 626, doi:10.1038/s41467-017-00729-8.
16. Théry, C.; Witwer, K.W.; Aikawa, E.; Alcaraz, M.J.; Anderson, J.D.; Andriantsitohaina, R.; Antoniou, A.; Arab, T.; Archer, F.; Atkin-Smith, G.K.; et al. Minimal information for studies of extracellular vesicles 2018 (MISEV2018): a position statement of the International Society for Extracellular Vesicles and update of the MISEV2014 guidelines. *J. Extracell. Vesicles* **2018**, *7*, doi:10.1080/20013078.2018.1535750.
17. Eguchi, T.; Sogawa, C.; Okusha, Y.; Uchibe, K.; Iinuma, R.; Ono, K.; Nakano, K.; Murakami, J.; Itoh, M.; Arai, K.; et al. Organoids with cancer stem cell-like properties secrete exosomes and HSP90 in a 3D nanoenvironment. *PLoS ONE 2018* **2018**, *13*.
18. Taha, E.A.; Ono, K.; Eguchi, T. Roles of extracellular HSPs as biomarkers in immune surveillance and immune evasion. *Int. J. Mol. Sci.* **2019**, *20*, doi:10.3390/ijms20184588.
19. Eguchi, T.; Sogawa, C.; Ono, K.; Matsumoto, M.; Tran, M.T. Cell Stress Induced Stressome Release Including Damaged Membrane Vesicles and Extracellular HSP90 by Prostate Cancer Cells. *Cells* **2020**, *9*.
20. Ono, K.; Sogawa, C.; Kawai, H.; Tran, M.T.; Taha, E.A.; Lu, Y.; Oo, M.W.; Okusha, Y.; Okamura, H.; Ibaragi, S. Triple knockdown of CDC37, HSP90-alpha and HSP90-beta diminishes extracellular vesicles-driven malignancy events and macrophage M2 polarization in oral cancer. *J. Extracell. vesicles* **2020**, *9*, 1769373, doi:10.1080/20013078.2020.1769373.
21. Witwer, K.W.; Buzás, E.I.; Bemis, L.T.; Bora, A.; Lässer, C.; Lötvall, J.; Nolte-'t Hoen, E.N.; Piper, M.G.; Sivaraman, S.; Skog, J.; et al. Standardization of sample collection, isolation and analysis methods in extracellular vesicle research. *J. Extracell. Vesicles* **2013**, *2*, doi:10.3402/jev.v2i0.20360.
22. Zaborowski, M.P.; Cheah, P.S.; Zhang, X.; Bushko, I.; Lee, K.; Sammarco, A.; Zappulli, V.; Maas, S.L.N.; Allen, R.M.; Rumde, P.; et al. Membrane-bound Gaussia luciferase as a tool to track shedding of membrane proteins from the surface of extracellular vesicles. *Sci. Rep.* **2019**, *9*, 1–16, doi:10.1038/s41598-019-53554-y.
23. Böing, A.N.; van der Pol, E.; Grootemaat, A.E.; Coumans, F.A.W.; Sturk, A.; Nieuwland, R. Single-step isolation of extracellular vesicles by size-exclusion chromatography. *J. Extracell. Vesicles* **2014**, *3*, doi:10.3402/jev.v3.23430.
24. Lai, C.P.; Kim, E.Y.; Badr, C.E.; Weissleder, R.; Mempel, T.R.; Tannous, B.A.; Breakefield, X.O. Visualization and tracking of tumour extracellular vesicle delivery and RNA translation using multiplexed reporters. *Nat. Commun.* **2015**, *6*, 1–12, doi:10.1038/ncomms8029.

25. Fujiwara, T.; Eguchi, T.; Sogawa, C.; Ono, K.; Murakami, J.; Ibaragi, S.; ichi Asaumi, J.; Calderwood, S.K.; Okamoto, K.; ichi Kozaki, K. Carcinogenic epithelial-mesenchymal transition initiated by oral cancer exosomes is inhibited by anti-EGFR antibody cetuximab. *Oral Oncol.* **2018**, *86*, 251–257, doi:10.1016/j.oraloncology.2018.09.030.
26. Grubisic, Z.; Rempp, P.; Benoit, H. A universal calibration for gel permeation chromatography. *J. Polym. Sci. Part B Polym. Lett.* **1967**, *5*, 753–759, doi:10.1002/pol.1967.110050903.
27. Monguió-Tortajada, M.; Gálvez-Montón, C.; Bayes-Genis, A.; Roura, S.; Borràs, F.E. Extracellular vesicle isolation methods: rising impact of size-exclusion chromatography. *Cell. Mol. Life Sci.* **2019**, *76*, 2369–2382, doi:10.1007/s00018-019-03071-y.
28. Gámez-Valero, A.; Monguió-Tortajada, M.; Carreras-Planella, L.; Franquesa, M.; Beyer, K.; Borràs, F.E. Size-Exclusion Chromatography-based isolation minimally alters Extracellular Vesicles' characteristics compared to precipitating agents. *Sci. Rep.* **2016**, *6*, 1–9, doi:10.1038/srep33641.
29. Lai, C.P.; Kim, E.Y.; Badr, C.E.; Weissleder, R.; Mempel, T.R.; Tannous, B.A.; Breakefield, X.O. Visualization and tracking of tumour extracellular vesicle delivery and RNA translation using multiplexed reporters. *Nat. Commun.* **2015**, *6*, 7029, doi:10.1038/ncomms8029.
30. Furuta, K.; Eguchi, T. Roles of HSP on Antigen Presentation. In *Heat Shock Proteins*; Asea, A.A.A., Kaur, P., Eds.; Springer, Dordrecht, 2020.
31. Ono, K.; Eguchi, T.; Sogawa, C. HSP-enriched properties of extracellular vesicles involve survival of metastatic oral cancer cells. *J. Cell. Biochem.* **2018**, *119*, 7350–7362, doi:10.1002/jcb.27039.
32. Okusha, Y.; Eguchi, T.; Tran, M.T.; Sogawa, C.; Yoshida, K.; Itagaki, M.; Taha, E.A.; Ono, K.; Aoyama, E.; Okamura, H.; et al. Extracellular vesicles enriched with moonlighting metalloproteinase are highly transmissive, pro-tumorigenic, and trans-activates cellular communication network factor (Ccn2/ctgf): CRISPR against cancer. *Cancers (Basel).* **2020**, *12*, doi:10.3390/cancers12040881.
33. Namba, Y.; Sogawa, C.; Okusha, Y.; Kawai, H.; Itagaki, M.; Ono, K.; Murakami, J.; Aoyama, E.; Ohyama, K.; Asaumi, J.I.; et al. Depletion of lipid efflux pump ABCG1 triggers the intracellular accumulation of extracellular vesicles and reduces aggregation and tumorigenesis of metastatic cancer cells. *Front. Oncol.* **2018**, *8*, 1–16, doi:10.3389/fonc.2018.00376.
34. Sogawa, C.; Eguchi, T.; Tran, M.T.; Ishige, M.; Trin, K.; Okusha, Y.; Taha, E.A.; Lu, Y.; Kawai, H.; Sogawa, N.; et al. Antiparkinson drug benztropine suppresses tumor growth, circulating tumor cells, and metastasis by acting on SLC6A3/dat and reducing STAT3. *Cancers (Basel).* **2020**, *12*, doi:10.3390/cancers12020523.
35. Kalluri, R.; LeBleu, V.S. The biology, function, and biomedical applications of exosomes. *Science* **2020**, *367*, doi:10.1126/science.aau6977.
36. Ono, K.; Eguchi, T.; Sogawa, C.; Calderwood, S.K.; Futagawa, J.; Kasai, T.; Seno, M.; Okamoto, K.; Sasaki, A.; Kozaki, K. ichi HSP-enriched properties of extracellular vesicles involve survival of metastatic oral cancer cells. *J. Cell. Biochem.* **2018**, *119*, 7350–7362, doi:10.1002/jcb.27039.
37. Vickers, K.C.; Palmisano, B.T.; Shoucri, B.M.; Shamburek, R.D.; Remaley, A.T. MicroRNAs are transported in plasma and delivered to recipient cells by high-density lipoproteins. *Nat. Cell Biol.* **2011**, *13*, 423–435, doi:10.1038/ncb2210.
38. B., S.J. What Are We Looking At? Extracellular Vesicles, Lipoproteins, or Both? *Circ. Res.* **2017**, *121*, 920–922, doi:10.1161/CIRCRESAHA.117.311767.
39. Karimi, N.; Cvjetkovic, A.; Jang, S.C.; Crescitelli, R.; Hosseinpour Feizi, M.A.; Nieuwland, R.; Lötvall, J.; Lässer, C. Detailed analysis of the plasma extracellular vesicle proteome after separation from lipoproteins. *Cell. Mol. Life Sci.* **2018**, *75*, 2873–2886, doi:10.1007/s00018-018-2773-4.
40. Kowal, J.; Arras, G.; Colombo, M.; Jouve, M.; Morath, J.P.; Primdal-Bengtson, B.; Dingli, F.; Loew, D.; Tkach, M.; Théry, C. Proteomic comparison defines novel markers to characterize heterogeneous populations of extracellular vesicle subtypes. *Proc. Natl. Acad. Sci. U. S. A.* **2016**, *113*, E968–E977, doi:10.1073/pnas.1521230113.
41. Lu, Y.; Eguchi, T. HSP Stimulation on Macrophages and Dendritic Cells Activates Innate Immune System. In *Heat Shock Proteins*; A.A.A.Asea, K.Punit, Eds.; Springer, Dordrecht: Dordrecht, 2020; pp. 1–15.

42. Eguchi, T.; Ono, K.; Kawata, K.; Okamoto, K.; Calderwood, S.K. Regulatory Roles of HSP90-Rich Extracellular Vesicles. In *Heat Shock Protein 90 in Human Diseases and Disorders*; Asea, A.A.A., Kaur, P., Eds.; Cham, Swizerland: Springer Nature: Cham, 2019; pp. 3–17 ISBN 978-3-030-23158-3.
43. Eustace, B.K.; Sakurai, T.; Stewart, J.K.; Yimlamai, D.; Unger, C.; Zehetmeier, C.; Lain, B.; Torella, C.; Henning, S.W.; Beste, G.; et al. Functional proteomic screens reveal an essential extracellular role for hsp90 alpha in cancer cell invasiveness. *Nat. Cell Biol.* **2004**, *6*, 507–514, doi:10.1038/ncb1131.
44. Schroder, K.; Hertzog, P.J.; Ravasi, T.; Hume, D.A. Interferon-gamma: an overview of signals, mechanisms and functions. *J. Leukoc. Biol.* **2004**, *75*, 163–189, doi:10.1189/jlb.0603252.
45. Murshid, A.; Eguchi, T.; Calderwood, S.K. Stress proteins in aging and life span. *Int. J. Hyperth.* **2013**, *29*, 442–447, doi:10.3109/02656736.2013.798873.
46. Eguchi, T.; Lang, B.; Murshid, A.; Prince, T.; Gong, J.; Calderwood, S. Regulatory Roles for Hsp70 in Cancer Incidence and Tumor Progression. In *Frontiers in Structural Biology*; Galigniana, M.D., Ed.; Bentham Science: Dordrecht, 2018; pp. 1–22 ISBN 9781681086156.
47. Goughnour, P.; Park, M.; Kim, S.; Jun, S.; Yang, W.S.; Chae, S.; Seongmin, C.; Song, C.; Lee, J.-H.; Hyun, J.; et al. Extracellular vesicles derived from macrophage display glycyl-tRNA synthetase 1 exhibits anti-cancer activity. *J. Extracell. Vesicles* **2020**, *10*, e12029, doi:10.1002/jev2.12029.
48. Park, M.C.; Kang, T.; Jin, D.; Han, J.M.; Kim, S.B.; Park, Y.J.; Cho, K.; Park, Y.W.; Guo, M.; He, W.; et al. Secreted human glycyl-tRNA synthetase implicated in defense against ERK-activated tumorigenesis. *Proc. Natl. Acad. Sci. U. S. A.* **2012**, *109*, E640-7, doi:10.1073/pnas.1200194109.